

## THE INFLUENCE OF ELECTROCONVECTION ON THE EFFICIENCY OF FINNED AIR COOLERS UNDER CONDITION OF FROST FORMATION

FATHY I. ABDEL AAL,  
Mechanical Power Dept., Faculty of Engineering and Tech.,  
Suez Canal Univ., A.R.E.

تأثير الحمل الكهربى على كفاءة مبخرات الهواء الجبرية ذات الريش تحت ظروف تكون الثلج

الخلاصة :

من أهم المشاكل التى تقابل علماء التبريد فى تصميم المبخرات هو تكون الثلج على أسطح هذه المبخرات أثناء التشغيل ، وما يترتب على ذلك من انخفاض فى الكفاءة ، وخاصة إذا كانت هذه المبخرات من النوع ذات الريش ، فبملا الثلج الفراغات التى بين هذه الريش فيزيد من مقاومة الايرودينامى لجريان الهواء ، فيقل بذلك معامل انتقال الحرارة وسعة التبريد ، وقد تناولت أبحاث كثيرة لمحاولة حل هذه المشكلة وذلك بالتعديل فى تصميم المبخرات .

فى هذا البحث دراسة عملية من تأثير الحمل الكهربى على كفاءة مبخرات غرف التبريد عند درجة حرارة (مفر) - (٢- )م<sup>٥</sup> .

وتتلخص الإضافات فى هذا البحث فيما يلى :

- ١- لجميع ظروف التشغيل استخدام الحمل الكهربى يزيد من كفاءة المبخرات إذا ما قورن بالتشغيل العادى للمبخر (بدون حمل كهربى) دون أى تعديل فى تصميم المبخر .
- ٢- تأثير الرطوبة النسبية وشدة المجال الكهربى على تكون سمك طبقة الثلج وأيضا على مقاومة الايرودينامى لحركة الهواء خلال ريش المبخر .
- ٣- تأثير شدة المجال الكهربى والرطوبة النسبية على معامل انتقال الحرارة وسعة التبريد للمبخر .
- ٤- فى هذا البحث اقترحت معادلة يمكن استخدامها لحساب كل من سمك طبقة الثلج ، سعة التبريد ومعامل انتقال الحرارة فى كل الظروف المتغيرة للتشغيل (الرطوبة النسبية - زمن التشغيل ) وذلك عند تصميم المبخرات التى تعمل فى ظروف الحمل الكهربى أو بدونه .

### Abstract

The influence of electro-convection with different parameters of electric field intensity on the air cooler efficiency under conditions of frost formation was studied. The electroconvective

air flow was faster as compared to the cooler operation without electro-convection. The higher the relative air humidity and the intensity of the electric field, the greater the effect of electro-convection upon the external heat exchange of the air cooler.

An equation is suggested for the estimation of frost thickness, specific heat flow and coefficient of heat transfer, and thus could be used in designing air coolers operating under electro-convective heat exchange.

#### Notations

- A - Coefficient accounting for the quality of heat-exchange surface = 0.0113;
- C - Coefficient of the heat flow sensor, (W/mV m<sup>2</sup>);
- d<sub>eq</sub> - Equivalent diameter of the finned surface, (m);
- d<sub>p</sub> - Tube diameter, (m);
- E - Electric field intensity, (V/m);
- e - Sensor reading, (mV);
- K - Overall coefficient of heat transfer, (W/m<sup>2</sup>K);
- L - Depth of the working surface of the air cooler, (m);
- q<sub>f</sub> - Specific heat flow, (W/m<sup>2</sup>);
- R<sub>fr</sub> - Frost thermal resistance, (m<sup>2</sup>.K/W);
- V<sub>a</sub> - Air velocity, (m/s);
- V<sub>a,Pa</sub> - Air mass velocity at the free area of the apparatus, (kg/s . m<sup>2</sup>);
- τ - Time, (h);
- ΔP - Change in the aerodynamic resistance of the air cooler, (Pa);
- t<sub>a</sub> - Air average temperature of refrigerated chamber, (°C);
- t<sub>s</sub> - Average temperature of the finned surface of an air cooler (°C);
- S<sub>p</sub> - Tube pitch, (mm);
- S<sub>f</sub> - Finning pitch, (mm);
- δ<sub>f</sub> - Fin thickness, (m);
- α - Coefficient of heat transfer (W/m<sup>2</sup>. K);
- φ - Relative air humidity, (%);
- δ<sub>fr</sub> - Frost thickness, (mm).

#### Subscripts

- i - Sensor number;
- E - In electric field;
- O - Without electric field.

#### 1- INTRODUCTION

The efficiency of operation of a cooling system, to a great extent, depends on frost formation on the surface of heat exchangers. The mechanism of frost formation, and its influence

upon air coolers have been a subject of several investigations (1-11). However, due to complexity of this non-stationary process, up till now there are no analytical relations solving this practical problem. Moreover coefficients of thermal conductivity and density involved vary with time and frost thickness, are interrelated and depend on the conditions under which frost and its crystallographic structure have been formed. Therefore, in many cases the experimental approach is the only possible mean to explore complicated heat exchange processes during frost formation. Data on frost deposition on finned surfaces of air coolers in air-conditioning systems and in refrigerated food storage rooms, are very scarce. Interesting work in this respect (1-4 & 6-11) have shown frost distribution on fins and elucidated problems connected with air cooler operation. Other investigations (6, 9 & 10) have revealed certain peculiarities in the dynamic of frost growth under practical operation conditions.

The nature of frost deposition on the finned surface of air coolers has been described as follows (1-4, 6-8 & 11). Initially, tube surface is most intensively frosted. Fin frosting starts at the bottom, then extends upwards. There after as the temperature of finned surface equalizes frost deposits evenly on the surface with equal thickness throughout; in case the air moisture content is high frost thickness grows more intensively.

Heat exchange in finned air coolers, has been studied through the overall coefficient of heat transfer  $K$  which involved heat resistances (1, 8 & 11). The results obtained have been presented in relation to either the service time or the amount of frost deposited on the surface, therefore in most cases they were incompatible. Studies (1-3, 5, 7 & 11) on the character that the nature of changes in the coefficient of heat transfer  $\alpha$  for all finned surfaces indicated that it was of the same type. At the beginning, when individual crystals appear on the heat exchange surface and air flow turbulization increased, the external heat exchange is intensified and  $\alpha$ -values grew up. Further, the inter-crystal space decreased, heat transmission occurred as a result of frost thermal conduction and convection in closed pores of the air.  $\alpha$  markedly decreased. As time passed, the frost became compacted, its thermal conduction rose and the rate of  $\alpha$  decrease slowed down.

Some available data (6, 9 & 10) indicate that frost formation contributes to a higher aerodynamic resistance rather than to deterioration of heat characteristics of the apparatus. Thus, in the air coolers operating in refrigerated meat chambers the overall heat transfer coefficient decreases by 25-30% and the aerodynamic resistance increases by 2.5-3 times.

For raising the efficiency of air coolers under frost formation conditions. Several authors (6, 9 & 10) suggest intermediate thawing which, in the opinion of some of them (9), increases significantly the aerodynamic resistance and, in the opinion of

some others (6 & 10) reduces specific heat flow. Thus, it has been shown that (6) the aerodynamic resistance in some cases reached 300-400 Pa by the 7th hour of meat refrigeration. This represents the maximum value which disturbs the normal operation of axial fans and necessitates air cooler thawing. On the other hand to obtain the specific heat flow of 116 W/m<sup>2</sup>, it is recommended (10) to thaw the cooler at frost thickness of 2.5 to 3 mm which is formed within 3-4 hours, i.e., twice or thrice during a refrigeration cycle.

Again, it has been demonstrated (9) that at an air relative humidity of 92-100% the aerodynamic resistance of an air cooler, having a cast bimetallic surface, was by 1.5-2 times lower as compared to coolers operating in refrigerated meat rooms (6 & 10), since by the end of the cycle the aerodynamic resistance reached 120-200 Pa; this offers a possibility of lowering the consumed power of the electric motor and of improving heat characteristics. The disadvantage of air coolers of this type is the difficulty of making a cast bimetallic surface (casting at 150 x 10<sup>5</sup> Pa).

Air cooler operation with frost deposition under conditions of electroconvection allows to intensify heat exchange, primarily due to the slower frost deposition on the heat exchange surface and to the additional acceleration of the air flow in the free area of the air cooler (2). The results published on frost formation on air cooler surfaces contain certain aspects of the processes, but they are of particular character and can not be applied to all the conditions of operation of finned air coolers of any designs.

The purpose of the present work is to study a possibility of raising the operation efficiency of air coolers by using electroconvective air flow in case of food refrigeration and refrigerated storage. In particular the study included the effect of frost on specific heat flow, heat transfer coefficient, air flow rate at the free area of an air cooler, as well as on the aerodynamic resistance of the heat exchange surface during operation with or without electroconvection; as an equation is derived to calculate frost thickness and heat transfer coefficient from the air side at different operation times of the apparatus in relation to operation conditions.

## 2- EXPERIMENTAL PROCEDURE AND METHODS OF MEASUREMENT

The experimental stand (Fig. 1) previously elaborated by the present author (2), was used to study the heat exchange and aerodynamics of a typical air cooler; the latter had a surface area of 4.3 m<sup>2</sup>, the finning pitch 12 and 9 mm along the air flow. The cooler was a part of a low-temperature display-case working with frost formation in electroconvective air flow. The present experiments were carried out at 0 to -2°C in the refrigerated chamber and R.H.  $\varphi$  of (73-76), (84-87) and (95-98) %.

At the air inlet of the cooler an electric field was developed with an average intensity  $E$  of  $6.8 \times 10^5$ ,  $7.2 \times 10^5$ ,  $7.7 \times 10^5$  and  $8.0 \times 10^5$  V/m. For comparison experiments were first performed without electric field,

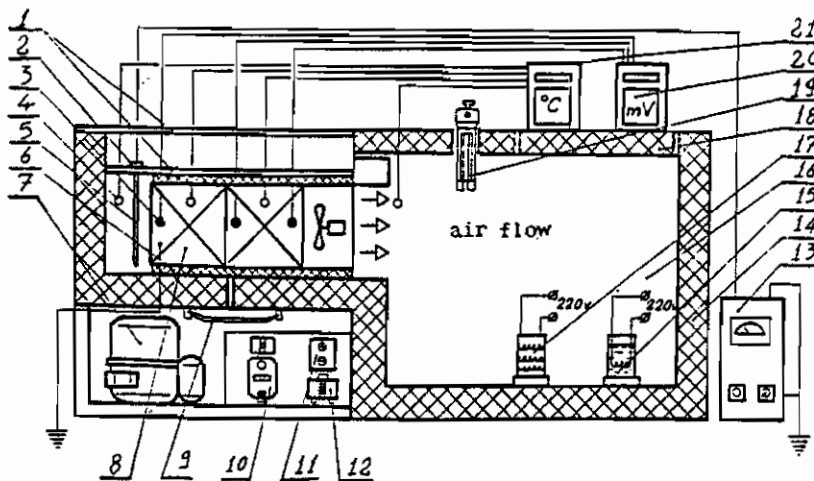


Fig. 1. A diagram of the experimental stand:

1- glass window; 2- fluoroplastic; 3- heat flow sensors;  
 4- thermocouples; 5- high-voltage electrode;  
 6- rubber seal; 7- compressor-condenser; 8- air cooler  
 9- tray for condensate; 10- switchboard; 11- time and  
 temperature relay; 12- thermorelay; 13- rectifier  
 14- thermoinsulator; 15- steam generator; 16- cooling  
 chamber; 17- electric heater; 18- movable wings;  
 19- psychrometer; 20- millivoltmeter; 21- potentiometer.

Before the experiment the refrigerating unit and steam generator of the stand were switched on, temperature and humidity in the chamber were adjusted to the pre-set level, and then the refrigerating unit and the steam generator were switched off, the finned surface was thawed with a 400-W tubular electric heater. It should be noted that for the period the chamber reached the pre-set conditions (not longer than 40 min.), frost thickness was insignificant and it was removed with the electric heater within 3 minutes. After thawing the high-voltage electrode was fed with a given potential, and the air cooler started working, the inlet air velocity  $V_a$  was 0.82 m/s. The required air temperature and relative humidity throughout the cycle were ensured with the electro-heater and the steam generator connected with the power

line through autotransformers. A continuous operation cycle of the air cooler with and without electroconvection with 8 hours.

Fourty-five chromel-copel thermocouples of 0.2 mm diameter, were used to measure the temperature of finned surface of the air cooler and of the air inside the chamber. The thermocouples were distributed as follow: 36 for the air cooler, 4 for recording the air temperature (2 at the inlet and 2 at the outlet) and 5 for the air inside the chamber.

The thermocouples used to measure the temperature of the air cooler surface at four sections along the air flow (one at the inlet, two at the middle and one at the outlet). In each section the temperature of tube wall was measured at three points; temperature of fin surface was recorded at two points along the three radii of each section as shown in Figure 2. Indication of the termocouples was attained with aid of a potentiometer.

The temperature in chamber was monitored by a laboratory mercury thermometer with a rang from  $-30^{\circ}\text{C}$  to  $+20^{\circ}\text{C}$ .

The specific heat load of the air cooler was measured by three heat flow sensors (connected to a millivoltemeter) located at the inlet, middle and the outlet along the air flow direction.

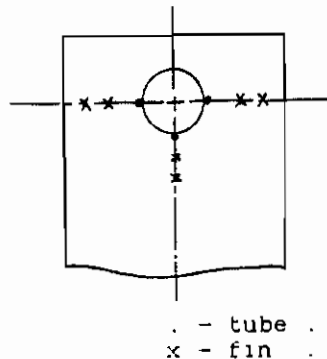


Fig. 2 Location of thermocouples

The outlet air velocity was measured by an anemometer, while the velocity of the air between fins was measured by an air velocity-temperature meter. Frost thickness on the surface of the air cooler was measured by a scale and checked by using a suitable photographic technique.

The relative air humidity in the chamber was measured with an aspiration psychrometer.

Instruments used and their specification are listed in table 1.

### 3. PROCESSING OF THE EXPERIMENTAL DATA

The values for specific heat flow to the surface of the air cooler  $q_F$  were found from the expression:

$$q_F = C_1 \cdot e_1, \text{ (W/m}^2\text{)} \dots\dots\dots(1)$$

Where,  $q_F$  is the average specific heat flow measured with heat flow meters located at the inlet, in the middle and at the outlet of the air cooler battery.

The heat transfer coefficient  $\alpha$  at the air cooler surface, at a given moment under different conditions, accounted for heat transmission from the air to the cooler surface through the frost layer was found from the equation,

$$\alpha = \frac{q_F}{t_a - t_s}, \text{ (W/m}^2\text{ K)} \dots\dots\dots(2)$$

Where,  $t_a$  ( $^{\circ}\text{C}$ ) is the arithmetic mean temperature at the inlet and the outlet of the cooler;  
 $t_s$  ( $^{\circ}\text{C}$ ) is the arithmetic mean of the temperatures recorded at different points of the finned surface.

The obtained data on the dynamics of frost deposition on the finned surface and associated air velocity  $V_a$  values allowed the determination of the aerodynamic resistance  $\Delta P$  of the air cooler from the following formula (2) :

$$\Delta P = 9.8A \cdot L/d_{eq} \cdot (V_a \cdot \rho_a)^{1.7}, \text{ (Pa)} \dots\dots\dots(3)$$

Where,

$$d_{eq} = \frac{2(S_D - d_D) (S_F - \delta_F)}{(S_D - d_D) + (S_F - \delta_F)}, \text{ (m)}.$$

Since  $d_{eq}$  and  $V_a$  change with the growth of frost due to the reduction of the free area for the air flow.  $\Delta P$  was relevantly recalculated for every frost thickness.

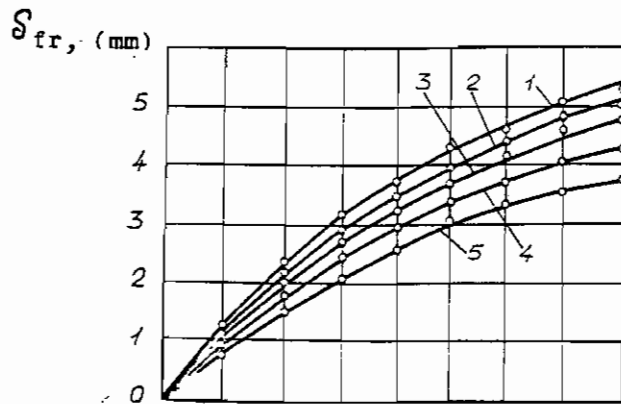
Table 1.

Instrument	Specifications				
	range	Accuracy %	Permissible error	division	coefficient $C_1$
1. Potentiometer (KSP)	-50°C to +50°C	0.5	-	0.5°C	-
2. Heat flow sensor					
1- inlet	-20°C to +120°C	-	±0.4%	-	135.0 W/(mV.m <sup>2</sup> )
2- middle	"	-	±0.4%	-	88.6 W/(mV.m <sup>2</sup> )
3- outlet	"	-	±0.4 %	-	153.0 W/(mV.m <sup>2</sup> )
3. Millivoltmeter (KSP)	0.0-10 mV	0.25	-	0.1 mV	-
4. Hg. Thermometer	-30°C to +20°C	-	±0.2°C	0.1°C	-
5. Anemometer	0.1-10 m/s	-	±0.1 m/s	-	-
6. Velocity-Temperature meter (GGA-45)	0.1-30 m/s	-	±0.05 m/s	0.1 m/s	-
7. Aspiration Psychrometer (MV-4M)	-	-	-	0.1°C	-

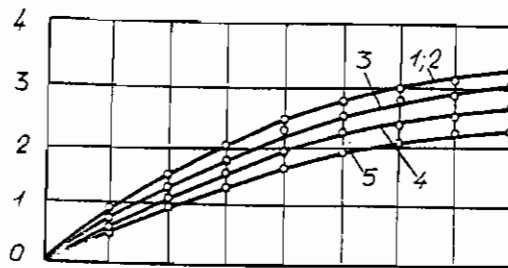
#### 4. RESULTS AND DISCUSSION

The experimental results showed that the most intensive was the frost deposition in the direction of the air flow through a row of finned tubes the character of changes in frost thickness at all humidities was similar over the entire surface of the apparatus. Fig. 3 presents the relation  $\delta_{fr} = f(\tau)$  for the first row of finned tubes. The effect of the field was most pronounced. There also a difference was observed in the rate of frost growth with electroconvection and without it. As seen from Fig. 3 the rate of frost growth in the air cooler was first of all determined by the relative air humidity, the intensity of the electric field and the position of the heat exchange surface. The higher the humidity, the greater the frost growth; superposition the higher the field intensity, the slower the frost growth (Fig. 4). The effect of electroconvection at  $\varphi = 95-98\%$  (Fig. 3a) was especially

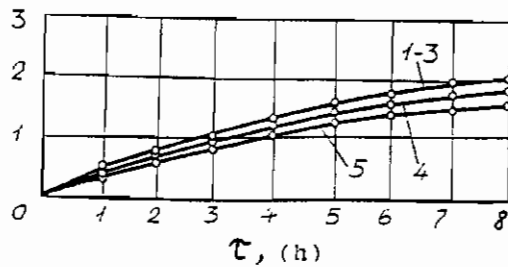




a -  $\varphi = 95 - 98\%$



b -  $\varphi = 84 - 87\%$



c -  $\varphi = 73 - 76\%$

Fig. 3. Frost formation on the first row of finned tubes of the air cooler during operation :

1-  $E = 0$ ; 2-  $E = 6.8 \times 10^5$  V/m; 3-  $E = 7.2 \times 10^5$  V/m;  
 4-  $E = 7.7 \times 10^5$  V/m; 5-  $E = 8.0 \times 10^5$  V/m.

pronounced, after 8 hr-continuous work the average frost thickness  $\delta_{cr}$  was 5.2 mm without electroconvection, i.e., it decreased by 4-30% less in case of electroconvection. It should be noted that the higher the field intensity, the lower the frost growth rate. At  $\varphi = 84-87\%$  the latter was reduced, however, frosting was most intensive without electroconvection (Fig. 3b). The  $\delta_{cr}$ -value with electroconvection decreased by 2-26%. The greatest amount of frost was deposited on the air cooler surface at  $\varphi = 73-76\%$  (Fig. 3c); higher potential resulted in a reduced frosting rate (by 0-23%).

When air relative humidity was reduced, frost growth increased by a relationship close to the linear (Fig. 3c).

The influence of the electric field intensity on frost formation rate could be attributed to the fact that as higher E-values increased the ion output of the high-voltage electrode increased, and therefore, more water particles, entering the interelectrode space, were charged and deposited onto the heat exchange surface as filaments carried away by air flow.

Fig. 4 illustrates the relative growth of frost layer in relation to the electric field intensity. With the increase of relative air humidity  $\varphi = 95-98\%$  (Curve 1) the efficiency of electroconvection rose, since the growth rate of relative frost thickness was greatly reduced. This was due, first of all, to the fact that at high humidities the frost structure was rough and this promoted directed frost formation. As humidity decreased, the roughness became lesser; thus at  $\varphi = 73-76\%$  powder-like frost of very uniform structure appeared: the frost thickness grew less intensively (Fig. 4, Curve 3). It was typical for all humidities that at the inlet of the air cooler the frost structure was more compact and uniform than at the outlet; this difference was most pronounced at  $\varphi = 95-98\%$ .

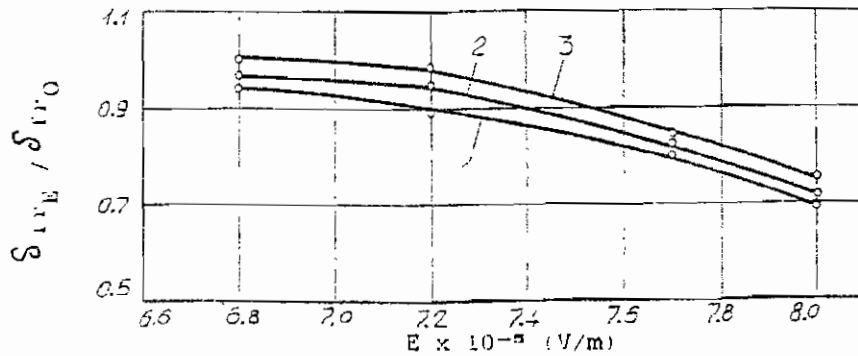


FIG. 4. Relative growth of frost  $\delta_{crE} / \delta_{cr0}$  within one operation cycle of the air cooler related to electric field intensity (E):  
 1-  $\varphi = 95-98\%$ ,      2-  $\varphi = 84-87\%$       3-  $\varphi = 73-76\%$



time slowed down. The following peculiarity of this time-related change at different relative air humidities should be noted: the time for the specific heat flow to reach its maximum became shorter at a higher relative air humidity; a greater value of humidity corresponded to a higher maximum of the heat flow (Fig. 5, Curve 1). This could be explained by that roughness of frost surface, being greatest at higher relative air humidity, caused a greater thermal resistance of the frost, and thereby resulted in a considerable reduction of the intensity of heat transfer.

The use of electroconvection inducing an "electric wind" effect and lowering the rate of frost growth allowed to raise the specific heat flow. Most pronounced was the electroconvection effect at a high relative air humidity (Fig. 5a). For example, a field having an intensity of  $8.0 \times 10^5$  V/m, increased the specific heat flow within a cycle at  $\varphi = 95-98\%$  by 19-21%, at  $\varphi = 84-87\%$  (Fig. 5b) by 12-14% and at  $\varphi = 73-76\%$  (Fig. 5c) by 9-10%.

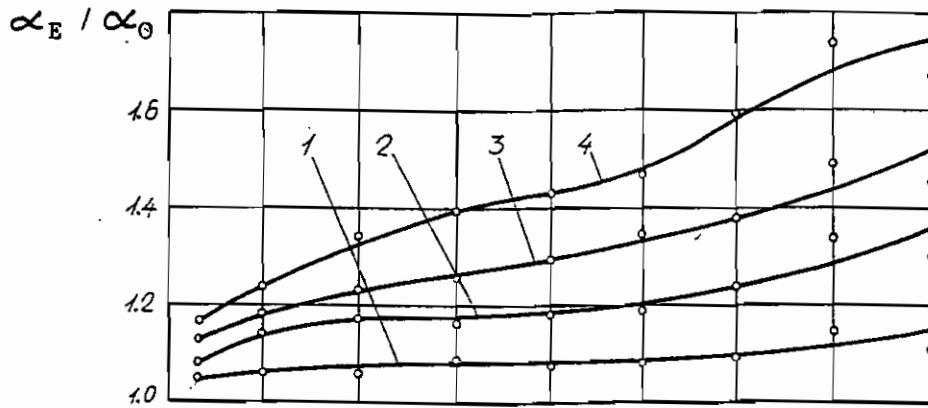
Fig. 6 demonstrates relative coefficient of heat transfer in relation to the operation time of the air cooler with or without electroconvection. Relationship  $\alpha_E / \alpha_0 = f(\tau)$  for different air humidities in the chamber were of the same character.

The value increased with operation time in all cases. However, the increase was proportional to the relative air humidity and the intensity of the electric field E. For example at  $\varphi = 95-98\%$  under conditions of electroconvection (Fig. 6a) the value of  $\alpha_E / \alpha_0$  increased by 1.05-1.15, 1.08-1.34, 1.17-1.74 times, respectively at  $E = 6.8 \times 10^5$ ,  $7.2 \times 10^5$  and  $8.0 \times 10^5$  V/m. At  $\varphi = 84-86\%$  (Fig. 6b) and at the same E-values,  $\alpha_E / \alpha_0$  increased by 1.0-1.08, 1.08-1.17 and 1.16-1.4 times, respectively. At  $\varphi = 73-76\%$  (Fig. 6c) and at  $E = 8.0 \times 10^5$  V/m it increased by 1.12-1.23 times.

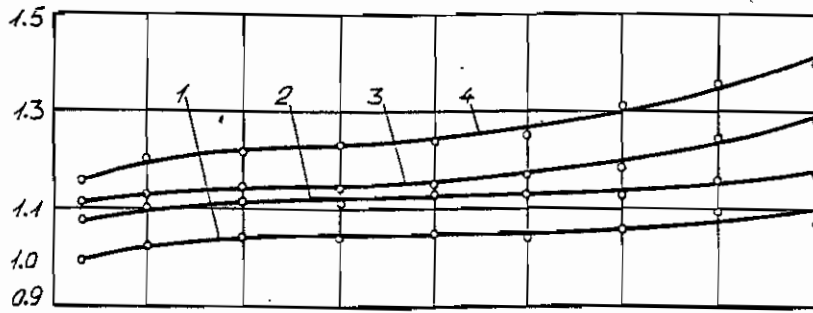
The increase of  $\alpha_E / \alpha_0$  with operation time. Could be due to the lower thermal resistance of frost thickness  $R_{fr}$  in case of electroconvection. However, at a lower air humidity,  $\varphi = 73-76\%$ , (Fig. 6c), frost thickness changed slightly with time and  $R_{fr}$  approached a constant value. Therefore,  $\alpha_E / \alpha_0$  of the air cooler slightly increased and tending to be constant.

The change of  $\alpha_E / \alpha_0$  in relation to the electric field intensity E developed by the electrode attachment, are given in Fig. 7, as the electric field intensity E increased and at all air humidities the influence of electroconvection on heat exchange was intensified due to the "electric wind" and to the slow frost formation on the heat exchange surface. The increase of  $\alpha_E / \alpha_0 = f(E)$  at  $t_a = \text{const.}$  was linear: the error of heat flow measurements did not exceed 4.1%. It is clear that the efficiency rose with the increase of relative air humidity in the chamber, the lowest value being recorded for  $\varphi = 73-76\%$ .

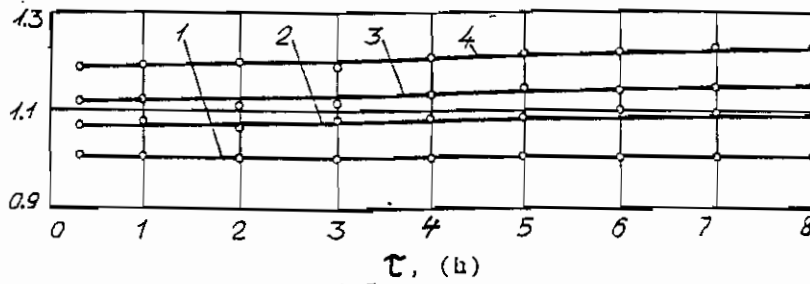
Fig. 8 presents the relation of air flow velocity at the free area of the air cooler with the intensity of the electric field E at different air humidities. The most intensive increase of



a -  $\phi = 95 - 98\%$



b -  $\phi = 84 - 87\%$



c -  $\phi = 73 - 76\%$

Fig. 6. Relative increase of heat transfer coefficients  $\alpha_E / \alpha_0$  in relation to air cooler operation time ( $\tau$ ):  
 1-  $E = 6.8 \times 10^5$  V/m;      2-  $E = 7.2 \times 10^5$  V/m;  
 3-  $E = 7.7 \times 10^5$  V/m;      4-  $E = 8.0 \times 10^5$  V/m.

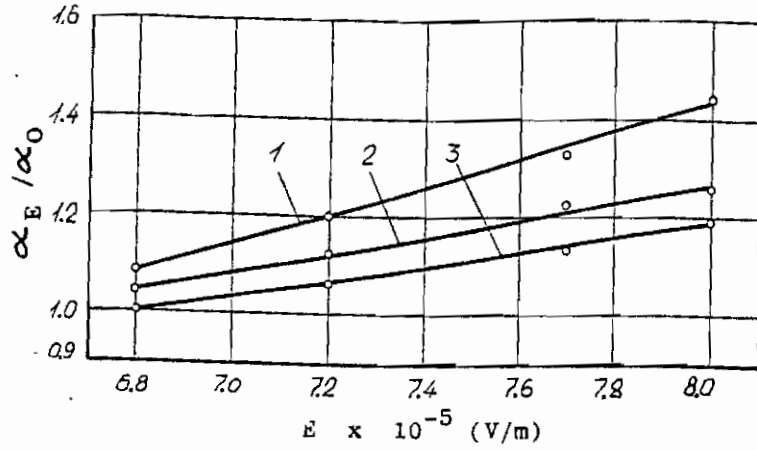


Fig. 7. Relative increase of the heat transfer coefficient  $\alpha_E / \alpha_0$  within one operation cycle of the air cooler in relation to electric field intensity. 1-  $\varphi = 95-98\%$ ; 2-  $\varphi = 84-87\%$ ; 3-  $\varphi = 73-76\%$ .

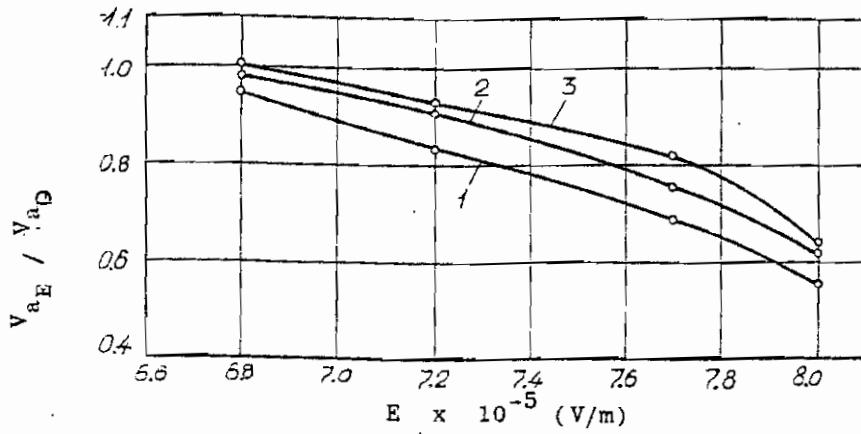


Fig. 8. Relative air velocity at the free area of the air cooler within one cycle of operation in relation to electric field intensity (E): 1-  $\varphi = 95-98\%$ ; 2-  $\varphi = 85-87\%$ ; 3-  $\varphi = 73-76\%$ .

the air flow with the increase of relative air humidity occurred in the first section of the air cooler, where the rate of frost growth and, hence, the narrowing of the arbitrary air passage were maximal. The electric field superposition decelerated frost formation and, in this way, reduced the rate of air flow at the free area of the apparatus. As seen from Fig. 8, for all the air humidities, the higher the field intensity  $E$ , the lower the relative air velocity  $V_{aE}/V_{a0}$  at the free area, noting that at a

higher air humidity  $V_{aE}/V_{a0}$  was reduced less intensively (Curve

1). This could be attributed to that at a decreased air humidity, when frost formation was slowed down, the efficiency of the influence of the electric field on the rate of  $V_{aE}/V_{a0}$  changes was

insignificant (Curve 3), and at  $E = 6.8 \times 10^5$  V/m the growth rate of  $V_{aE}/V_{a0}$  remained unchanged.

Changes of the air flow rate at the free area of the apparatus in the first section of the air cooler in case of 95-98% relative humidity are presented in Fig. 9, the air velocity at the free area of the cooler altered as follows: the initial frost layer ( $\delta_{fr} = 1.0-1.5$  mm) slightly accelerated the air flow in the cooler, then the velocity increased markedly and during the last hours of operation, when frost formation decreased, the air flow rate decreased. These peculiarities demonstrated themselves at a high air humidity. At lower air humidities, the air flow rate increased more evenly (Fig. 8, Curve 1).

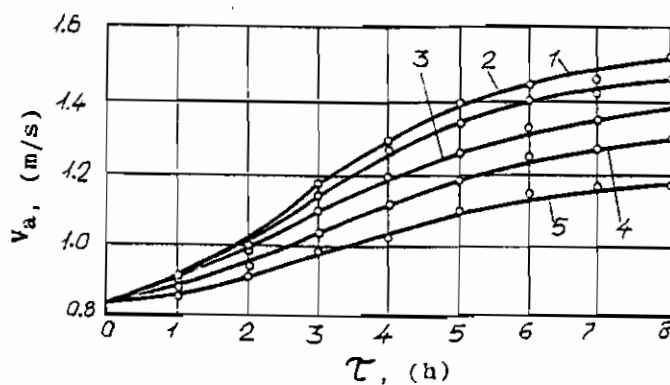


Fig. 9. Air velocity at the free area of the air cooler in relation to its operation time at relative air humidity  $\varphi = 95-98\%$ :  
 1-  $E = 0$ ;            2-  $E = 6.8 \times 10^5$  V/m;            3-  $E = 7.2 \times 10^5$  V/m;  
 4-  $E = 7.7 \times 10^5$  V/m;            5-  $E = 8.0 \times 10^5$  V/m.

The effect of electroconvection on the growth rate of aerodynamic resistance of the air cooler ( $\Delta P_E / \Delta P_0$ ) is demonstrated in Fig. 10. The maximal value of  $\Delta P_0$  was observed at  $\varphi = 95-98\%$ , the reason lied in the narrowing of the free area of the apparatus during frost formation. Decrease of growth rate of aerodynamic resistance of the air cooler accompanying the increase of electric field intensity, since the lowest value of  $\Delta P_E / \Delta P_0$ , for all humidities regimes was observed at  $E = 8 \times 10^5$  V/m. At 95-98% humidity the maximal electroconvection effect was observed, and at 73-76% and  $E = 6.8 \times 10^5$  V/m there was no effect at all.

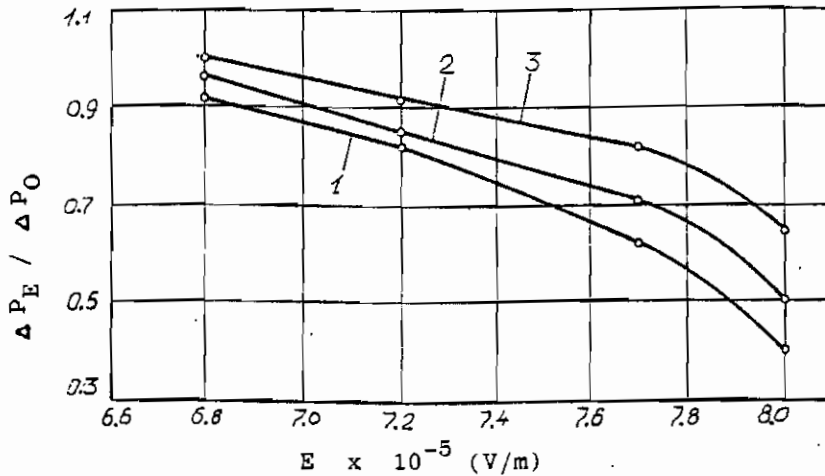


Fig. 10. Relative aerodynamic resistance of the air cooler  $\Delta P_E / \Delta P_0$  within one operation cycle in relation to electric field intensity:  
 1-  $\varphi = 95-98\%$ ;                      2-  $\varphi = 84-87\%$ ;                      3-  $\varphi = 73-76\%$ .

The character of changes of the aerodynamic resistance by time is shown in Fig. 11. It is clear that initially the aerodynamic resistance grew only slightly, then  $\Delta P$ -values greatly increased and by the end of the cycle the growth rate somewhat decreased; most vivid these changes were at  $\varphi = 95-98\%$ .

The processing of the experimental data in a computer allowed to derive operation as relations in the form of equation of nonlinear regression of the 3rd degree for determining frost thickness, the coefficient of heat transfer and specific heat flow :



$$\begin{aligned} \delta_{er}; \alpha; q_F = & B_1 + B_2 \tau + B_3 \tau^2 - B_4 \tau^3 + B_5 E + B_6 \tau E \\ & + B_7 E \tau^2 + B_8 E^2 + B_9 \tau E^2 + B_{10} E^3 + B_{11} \varphi \\ & + B_{12} \tau \varphi + B_{13} \varphi \tau^2 + B_{14} E \varphi + B_{15} \tau E \varphi \\ & + B_{16} \varphi E^2 + B_{17} \varphi^2 + B_{18} \tau \varphi^2 + B_{19} E \varphi^2 \\ & + B_{20} \varphi^3. \end{aligned}$$

Standard deviations are as follows :

- \*\* For  $\delta_{er}$ , 0.14 mm,
- \*\* For  $\alpha$ , 2.1 W/(m<sup>2</sup>.K),
- \*\* For  $q_F$ , 7.2 W/m<sup>2</sup>.

The values of obtained coefficients are given in table 2.

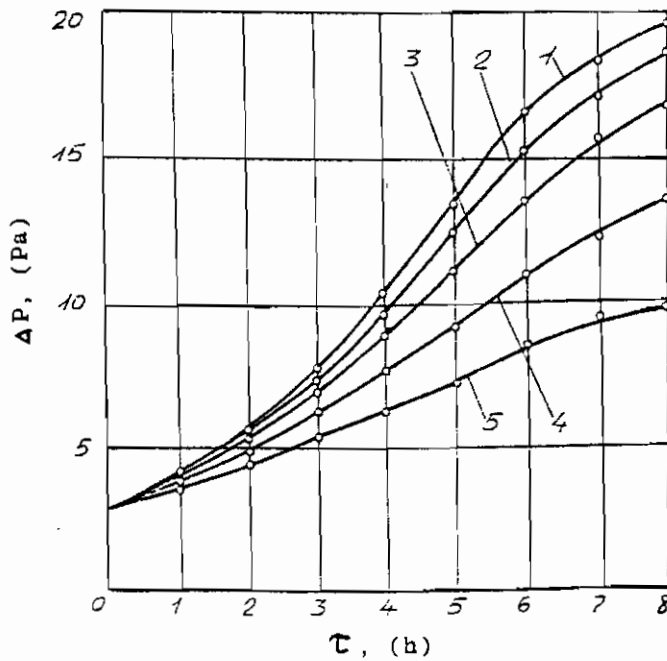


Fig. 11. Character of changes of the aerodynamic resistance of the air cooler within one operation cycle at  $\varphi = 95-98\%$ :  
 1-E = 0;            2-E = 6.8x10<sup>5</sup> V/m;            3-E = 7.2x10<sup>5</sup> V/m;  
 4-E = 7.7x10<sup>5</sup> V/m;            5-E = 8.0x10<sup>5</sup> V/m.

Table 2.

Coefficient	$\delta_{fr}$ , (mm)	$\alpha$ , (W/m <sup>2</sup> .K)	$q_F$ , (W/m <sup>2</sup> )
B <sub>1</sub>	-6.05	-5.03 . 10 <sup>2</sup>	7.58 . 10
B <sub>2</sub>	-2.59 . 10 <sup>-2</sup>	1.09 . 10 <sup>-1</sup>	4.29 . 10 <sup>-1</sup>
B <sub>3</sub>	2.53 . 10 <sup>-4</sup>	-4.28 . 10 <sup>-3</sup>	-1.46 . 10 <sup>-2</sup>
B <sub>4</sub>	-6.77 . 10 <sup>-6</sup>	-5.09 . 10 <sup>-6</sup>	-2.58 . 10 <sup>-7</sup>
B <sub>5</sub>	9.28 . 10 <sup>-11</sup>	-5.24 . 10 <sup>-9</sup>	-7.18 . 10 <sup>-9</sup>
B <sub>6</sub>	-2.15 . 10 <sup>-14</sup>	2.02 . 10 <sup>-13</sup>	9.01 . 10 <sup>-13</sup>
B <sub>7</sub>	-9.41 . 10 <sup>-6</sup>	-2.95 . 10 <sup>-2</sup>	1.46 . 10 <sup>-3</sup>
B <sub>8</sub>	1.62 . 10 <sup>-4</sup>	-5.25 . 10 <sup>-4</sup>	-2.16 . 10 <sup>-3</sup>
B <sub>9</sub>	8.43 . 10 <sup>-10</sup>	-6.22 . 10 <sup>-10</sup>	-3.41 . 10 <sup>-9</sup>
B <sub>10</sub>	-1.83 . 10 <sup>-6</sup>	3.03 . 10 <sup>-4</sup>	1.67 . 10 <sup>-6</sup>
B <sub>11</sub>	1.40 . 10 <sup>-1</sup>	2.01	1.11 . 10 <sup>-1</sup>
B <sub>12</sub>	2.04 . 10 <sup>-2</sup>	-9.38 . 10 <sup>-3</sup>	1.23 . 10 <sup>-1</sup>
B <sub>13</sub>	-7.42 . 10 <sup>-4</sup>	3.58 . 10 <sup>-3</sup>	4.27 . 10 <sup>-3</sup>
B <sub>14</sub>	1.51 . 10 <sup>-7</sup>	-3.10 . 10 <sup>-7</sup>	-2.10 . 10 <sup>-6</sup>
B <sub>15</sub>	-1.59 . 10 <sup>-9</sup>	7.29 . 10 <sup>-9</sup>	3.31 . 10 <sup>-8</sup>
B <sub>16</sub>	-6.46 . 10 <sup>-14</sup>	2.61 . 10 <sup>-13</sup>	1.40 . 10 <sup>-12</sup>
B <sub>17</sub>	-1.17 . 10 <sup>-3</sup>	1.66 . 10 <sup>-1</sup>	1.37 . 10 <sup>-2</sup>
B <sub>18</sub>	1.06 . 10 <sup>-5</sup>	-7.45 . 10 <sup>-4</sup>	-3.69 . 10 <sup>-3</sup>
B <sub>19</sub>	-9.70 . 10 <sup>-10</sup>	1.14 . 10 <sup>-9</sup>	1.15 . 10 <sup>-8</sup>
B <sub>20</sub>	5.36 . 10 <sup>-6</sup>	-1.31 . 10 <sup>-3</sup>	-5.79 . 10 <sup>-8</sup>

## 5. CONCLUSIONS

The use of electroconvective air flow in air coolers under conditions of frost formation allowed to prolong the time of continuous operation of the apparatus, to increase the average specific heat flow by 9-21% and the value of heat transfer coefficient by 5-45%, as well as to lower aerodynamic resistance by 1.1-2.0 times, depending on the parameters of the electric field and the operation conditions of air coolers, as compared to operation without electroconvection.

Also the power consumed by the fan electric motor during air cooler operation with electroconvection was reduced by 5-27%.

Relations have been derived for the estimation of  $\delta_{fr}$ ,  $\alpha$ ,  $q_F$ . These relations have accounted for the effect of  $\varphi$ ,  $E$  and  $\tau$  on these values, and thus they could be recommended in designing of air coolers.

## 6. ACKNOWLEDGEMENTS

I would like to express my thanks to the Dept. of Refrigerating Technique, Institute of Applied Biotechnology, Moscow, for assistance during research.

## 7. REFERENCES

1. Techepurnenko V.P., Khamadze O.I. and Melnikov P.I. A study in heat at exchange in air coolers used for food refrigeration. Kholodilnaya Tekhnica and Technologia, Kiev. 1983, N 36, pp. 124-128.
2. Fathy I. Abdel Aal. the influence of electroconvection on heat and mass exchange during air cooling in finned air coolers. -PSE Bulletin. Vol. 2, 1990. Faculty of Engineering, Port Said, Egypt.
3. Hayashi Y., Yuhara H. and Aoki K. Research of Frost Formation by Forced Convection. - Trans. ASME, 1976, V. 42, N 355, PP. 885-901.
4. Marinyuk B.T. Account of Thermal Resistance of Frost when calculating Heat - Exchange Apparatuses., -Kholodilnaya Tekhnica, Moscow, 1989, No. 4, PP. 30-32.
5. Ivanova V.S. Heat exchange of finned air coolers upon frost formation - Kholodilnaya Tekhnica, Moscow 1978, N. 11, PP. 57-61.
6. Sedneyev N.P. Gerasimov N.A. and Sergina I.V. Determination of thawing time of dry suspended air coolers. - Kholodilnaya Technica, Moscow 1979, N 1, PP. 35-36.
7. Tajima O. Frost formation on air cooler. - Refrigeration, Japan, 1978, V. 53, N 608, PP. 499-512.
8. Trammell G.J., Little D.C. and Killgore E.M. A study of frost formed on a plate held at sub-freezing temperatures. -ASHRAE, 1968, N 7, PP. 42-47.
9. Khamaladze O.I. Aerodynamic resistance of air coolers upon frost formation. -Kholodilnaya Tekhnica, Moscow 1985, N 3, PP. 25-28.
10. Yanushevsky V.I. Experience of the operation of air coolers of VOP and VOG Types at cold stores of the meat industry. -Kholodilnaya Tekhnica, Moscow 1977, N 12, PP. 46-48.
11. Yavnel V.K. On heat transfer through a frost layer. -Kholodilnaya Tekhnica, 1969, N 5, PP. 34-37.